Bulletin of Mathematical Biology (2001) **63**, 573–595
doi:10.1006/bulm.2001.0237
Available online at http://www.idealibrary.com on IDEAL®

Low Seasonal Temperatures Promote Life Cycle Synchronization

JANETTE L. JENKINS AND JAMES A. POWELL*
Department of Mathematics and Statistics,
Utah State University,
Logan,
Utah 84322-3900, U.S.A.

JESSE A. LOGAN AND BARBARA J. BENTZ
USDA Forest Service Forestry Sciences Lab,
Utah State University,
Logan,
Utah 84322-8000, U.S.A.

In this paper we discuss how seasonal temperature variation and life-stage specific developmental thresholds that cause quiescence can synchronize the seasonal development of exothermic organisms. Using a simple aging model it is shown that minimal seasonal temperature variation and periods of quiescence during extreme temperature conditions are sufficient to establish stable, univoltine ovipositional cycles. Quiescence induced by life-stage specific developmental thresholds, in fact, promotes synchronous oviposition and emergence. The mountain pine beetle, an important insect living in extreme temperature conditions and showing no evidence of diapause, invites direct application of this model. Simulations using mountain pine beetle parameters are used to determine temperature regimes for which stable ovipositional cycles exist.

1. INTRODUCTION

Synchrony and seasonality are essential to the survival and reproduction of many poikiliothermic organisms† (Zaslavski, 1988; Logan and Bentz, 1999). Specifically, the mountain pine beetle (*Dendroctonus ponderosae* Hopkins, MPB), an important organism in forest ecosystem successional dynamics, must emerge as an adult in the appropriate season in order to reproduce. Because their prey, conifers of the genus *Pinus*, have defenses against attack, MPB must attack trees *en masse* in order to successfully lay eggs (Raffa and Berryman, 1980; Raffa, 1988). This requires that the beetles not only emerge as adults at the right time of the year

*Author to whom correspondence should be addressed. *E-mail*: powell@math.usu.edu

†'Poikiliothermic' and 'Exothermic' are terms we use here to describe organisms whose body temperature is essentially that of their external environment, i.e., 'cold-blooded.'

0092-8240/01/030573 + 23 $35.00/0

(timing), but also that the beetles emerge essentially all at once (synchrony). Both appropriate timing and synchrony are required for an adaptive seasonality. A MPB generation usually completes in one year (univoltine[‡]) although 2 years may be required at higher elevations (semi-voltine). Observations indicate that, while eggs may be laid over a 2–3 month period of time, peak adult emergence typically occurs over a much shorter interval (Amman and Cole, 1983; Raffa, 1988). This suggests that MPB have some mechanism which helps synchronize their emergence.

Many insects use diapause to achieve seasonality. Diapause is a state in which development is suspended, which resets the thermal clock for poikiliothermic organisms (Tauber *et al*., 1986). This means that the life cycle is synchronized at this point and all the individuals are essentially the same age when some external stimulus releases the population from diapause. However, MPB show no evidence of diapause. Phenology of insects with no obvious seasonal timing mechanism, such as diapause, is under direct temperature control (Danks, 1987). Hence, temperature is a strong requisite for MPB and other such insects to simultaneously emerge at the appropriate time (Raffa and Berryman, 1980; Logan and Bentz, 1999; Logan and Powell, 2001).

Logan and Bentz (1999) developed a model to study direct temperature control as a mechanism for synchrony and seasonality in MPB. The model uses the median oviposition date as the first approximation of when a population of beetles will reach maturity and reproduce. The model is based on nonlinear growth curves previously parameterized by Logan (1988). Beginning a 'beetle' on every day of the year and running this model over many generations shows that after a few years, successive generations emerge either on a single day every year, a finite set of days, or a cycle (sometimes complex) of days (Logan and Bentz, 1999). The results of the model appear to be robust, suggesting that synchronization may occur for a range of realistic temperature cycles. This raises the question, in the absence of diapause what mechanisms promote seasonality?

Each life stage in MPB has a lower lethal threshold and a lower developmental threshold, either of which might enhance synchronization. The lower lethal threshold is a temperature below which the beetles cannot survive. The lower developmental threshold is a temperature below which beetles cannot develop, but remain in a quiescent state waiting for warmer temperatures as described by Bentz *et al*. (1991). The lethal threshold, which varies for each developmental life stage, could serve to synchronize emergence by culling those individuals born from eggs laid too late or too early. However, recent evidence indicates that lower lethal thresholds are typically not reached, especially during midwinter (Bentz and Mullen, 1999), and are therefore not likely to cause synchronization.

The developmental threshold may also promote synchrony and seasonality in insects without diapause. Newbold *et al*. (1994) illustrated this in the specific case

[‡]'Voltinism' refers to the number of generations an organism completes per year. Thus, uni-voltine organisms complete one generations per year, bi-voltine complete two generations per year and so forth.

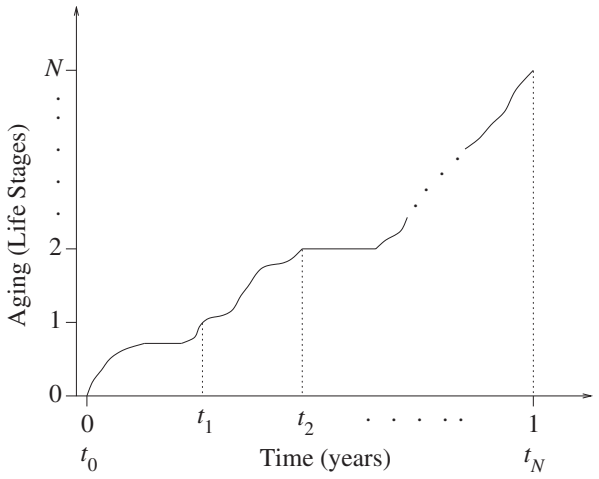

Figure 1. Univoltine aging for N life stages. The t_j's on the horizontal axis are the times at which the beetle changes from one life stage to another. Numbers on the vertical axis indicate which life stage is completed thus far. Flat portions of the curve indicate periods during which the beetle is in a quiescent state (temperatures are below threshold) and not developing.

of mayflies; Bentz *et al*. suggested quiescence as a synchronizing mechanism for oviposition of MPB in 1991, influenced by the earlier work of Amman (Amman and Cole, 1983). Gurney *et al*. (1992) demonstrated that development-free diapause in some life stage is sufficient to cause phase-locking with the seasonal temperature cycle in a theoretical two-stage organism, and expanded on their results in a series of other papers regarding two-stage organisms (Gurney *et al*., 1994; Grist and Gurney, 1995). Powell *et al*. (2000) showed that even in multi-stage organisms, actual quiescence is not required for synchronization, only the differential developmental dependence on temperature. In the current manuscript we will explore how the presence of multiple thresholds and a variety of possibilities for dormancy enhance seasonality in multi-stage organisms like MPB.

In a previous paper Powell *et al*. (2000) describe a linear caricature of Logan's model with simple seasonal temperature variations and linear developmental rate curves. It was shown that seasonal temperature swings alone are sufficient to establish seasonality in exothermic organisms. A mathematical *caveat* was that temperatures were required to remain *above* developmental thresholds, even though MPB live in environments with very cold temperatures. In this paper we extend the analysis to the realistic case in which temperatures can drop below developmental thresholds and insects remain quiescent for a period of time. This is a crucial extension for both mathematical and biological reasons. Biologically, most temperate zone insects experience annual temperatures below their developmental thresholds. Mathematically, when temperatures pass through thresholds, discontinuities in the developmental map are created. While the dynamics of continuous circle maps

is well understood, no corresponding body of knowledge exists for discontinuous maps. Our goal in this paper is to deduce sufficient conditions for the existence of univoltine oviposition cycles, even in the presence of these discontinuities. In the specific case of MPB we will compare these predictions with detailed simulations of seasonality.

In the next section a simplified mathematical development model is presented, focussing on the development of the median individual in each generation. We show that univoltine solutions exist and illustrate the synchronizing effect of lifestage specific developmental thresholds. This leads us to determine sufficient conditions for the existence of univoltine solutions for an organism with N life stages. Finally we examine temperature regimes that create voltinism using both linear and nonlinear developmental rate curves and predict regions of synchrony and seasonality for the mountain pine beetle.

2. MATHEMATICAL MODEL

The general developmental model for the 'age', or fraction of the jth life stage completed, $a_j(t)$, of the median individual can be written as

$$\frac{da_j}{dt} = R_j(T(t)), \qquad a_j(t_{j-1}) = 0.$$

The function $R_j(T)$ is the rate of aging, where t is time and $T(t)$ is the temperature at time t. The developmental age varies between 0 and 1, with t_j being the time of completion of the (j)th life stage and $a_j(t_j) = 1$ (see Fig. 1). Formally, one may write the solution for t_N, the date of adult emergence and oviposition, implicitly:

$$\begin{aligned}
1 &= \int_{t_0}^{t_1} R_1(T(t))\, dt, \\
1 &= \int_{t_1}^{t_2} R_2(T(t))\, dt, \\
&\vdots \\
1 &= \int_{t_{j-1}}^{t_j} R_j(T(t))\, dt, \\
&\vdots \\
1 &= \int_{t_{N-1}}^{t_N} R_N(T(t))\, dt. \qquad (1)
\end{aligned}$$

Analytically, finding a closed-form solution for t_N is not simple (or even possible) in general circumstances, but from a computational perspective one simply integrates to 1 repeatedly, saving the final result. For any given temperature regime,

t_N will depend on t_0—the time of the year during which the egg was laid; consequently we may think of t_N as a map from t_0 to the interval $[0, 1)$. Since every ovipositional date, t_0, generates at most one emergence date and time, t_N, we may write t_N as a function

$$t_N = G(t_0).$$

Temperatures are not constant in temperate regions. Taking t to be measured in years, with $t = 0$ at the average yearly minimum temperature (say January 30), a simple mathematical model for seasonal variation of temperature (Taylor, 1981) is

$$T(t) = T_0 - T_1 \cos(2\pi t). \tag{2}$$

In this equation T_0 is the yearly average temperature and T_1 is the size of the seasonal contribution to yearly temperature swings; that is, $2T_1$ is the temperature difference between the coldest and hottest parts of the year. The behavior of yearly temperature is *much* more complicated than this, but as has been shown by Powell *et al*. (2000), this minimal seasonality is enough to establish voltinism. Conversely, the additional terms needed to improve the accuracy of $T(t)$ are not, within reasonable limits, sufficient to destroy voltinism.

Ovipositional dates cycle from 0 to 1 and then repeat, so solutions for t_N are interpreted modulo 1. This creates the possibility for fixed points and strong seasonality; if $t_N = 1 + t_0$ then t_0 is an equilibrium solution for oviposition corresponding to a univoltine cycle. Similarly, if

$$t_N = m + t_0$$

then t_0 is an equilibrium solution for an $\frac{1}{m}$-voltine cycle.

Suppose $R_j(T)$ is the simplest possible linear temperature-dependent rate of development which includes thresholds,

$$R_j(T) = \max[0, r_j(T(t) - \theta_j)]. \tag{3}$$

For temperatures as in (2),

$$r_j(T(t) - \theta_j) = r_j[T_0 - \theta_j - T_1 \cos(2\pi t)]. \tag{4}$$

In (4), the parameters r_j and θ_j are stage-specific constants; r_j is the linear rate of development for temperatures above threshold and θ_j is the developmental threshold temperature for life stage j. In regions where MPB live the temperature is quite cold during much of the year, often below some developmental threshold (see Fig. 2). Analytically, it is cumbersome to carry the $\max[0, r_j(T - \theta_j)]$, so

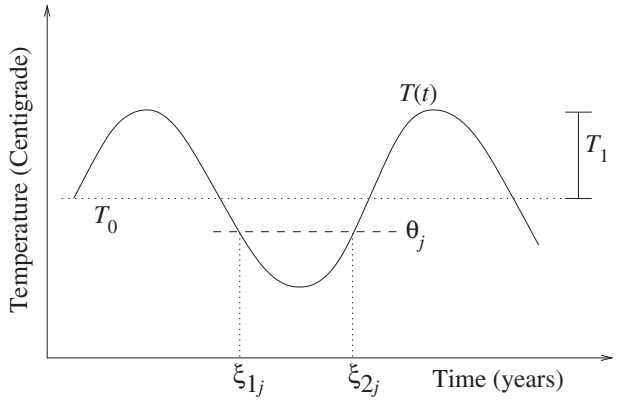

Figure 2. The temperature curve, $T(t) = T_0 - T_1 \cos(2\pi t)$, used in the model. T_0 is the mean annual temperature, T_1 is the size of the seasonal fluctuations, and θ_j is the developmental threshold for life stage j. For times between ξ_{1_j} and ξ_{2_j} the temperature is below the developmental threshold, that is, $(T_0 - T_1) < \theta_j$.

instead we elect to subtract out periods of time during which $R_j < 0$ in (1), that is, we express aging for life stage j as

$$1 = \int_{t_{j-1}}^{\xi_{1_j}} R_j(T(t))dt + \int_{\xi_{2_j}}^{t_j} R_j(T(t))dt = \int_{t_{j-1}}^{t_j} R_j(T(t))dt - \int_{\xi_{1_j}}^{\xi_{2_j}} R_j(T(t))dt. \tag{5}$$

The beginning of a quiescent period in life stage j is ξ_{1_j} and the end of the same quiescent period is ξ_{2_j}. Equation (5) can be rewritten as

$$1 = f_j(t_{j-1}, t_j) - \int_{\xi_{1_j}}^{\xi_{2_j}} R_j(T(t))dt, \tag{6}$$

with

$$f_j(t_{j-1}, t_j) \stackrel{\text{def}}{=} \left[(T_0 - \theta_j)(t_j - t_{j-1}) - \frac{T_1}{2\pi}(\sin(2\pi t_j) - \sin(2\pi t_{j-1})) \right] \tag{7}$$

and $\int_{\xi_{1_j}}^{\xi_{2_j}} R_j(T(t))dt$ expanded as

$$r_j \left[(T_0 - \theta_j)(\xi_{2_j} - \xi_{1_j}) - \frac{T_1}{2\pi}(\sin(2\pi\xi_{2_j}) - \sin(2\pi\xi_{1_j})) \right].$$

In the event that there is no quiescence, we set $\xi_{1_j} = \xi_{2_j}$. Suppose temperature is below the developmental threshold for life stage j (as in Fig. 2). To find the points at which the temperature equals the threshold, set

$$\theta_j = T_0 - T_1 \cos(2\pi\alpha_j).$$

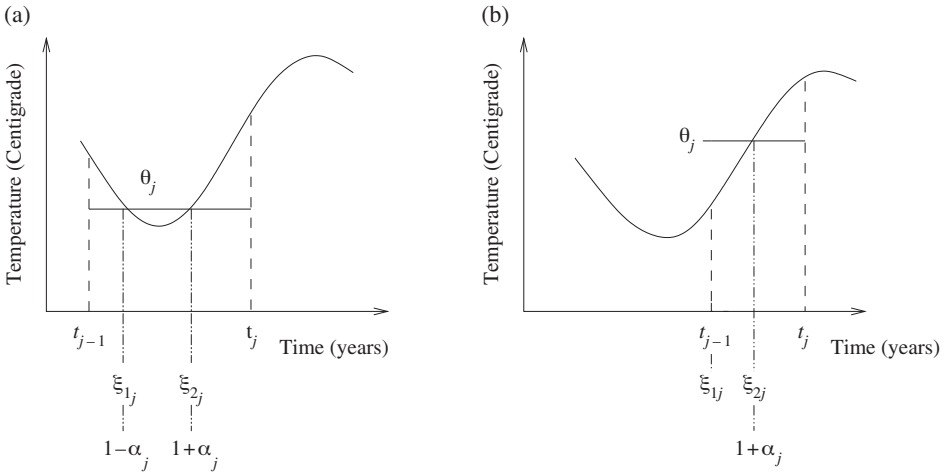

Figure 3. This figure shows two ways in which quiescence impacts developments. (a) (stop) shows the case where both endpoints of quiescence, ξ_{1_j} and ξ_{2_j}, are functions of α_j; (b) (speed bump) shows the case where the first endpoint, ξ_{1_j}, is the beginning of the life stage and the second endpoint, ξ_{2_j}, is a function of α_j.

Solving for α_j gives

$$\alpha_j = \frac{1}{2\pi}\cos^{-1}\left[\frac{T_0 - \theta_j}{T_1}\right]. \tag{8}$$

Due to the periodic temperature curve, critical points occur at $\pm\alpha_j$, $1 \pm \alpha_j$, $2 \pm \alpha_j, \ldots$, depending on what time of year development begins.

To see why we distinguish between α_j and ξ_j consider Fig. 3. For a beetle developing in life stage j, if the temperature goes below θ_j, then the beetle stops developing until the temperature rises above θ_j again. In this case zero aging begins and ends at two successive α_js, e.g., $-\alpha_j$ and α_j or $1-\alpha_j$ and $1+\alpha_j$ or $2-\alpha_j$ and $2+\alpha_j$ [see Fig. 3(a)], a situation we refer to as a 'stop'. If the thresholds are increasing between life stages $j-1$ and j, then the beetles could finish development of life stage $j-1$ and move into life stage j. However, if the temperature at t_{j-1} is below θ_j, then the beetles enter a quiescent state at the beginning of life stage j and remain so until the temperature rises above θ_j, at which time development for that life stage begins, a situation we refer to as a 'speed bump'. In this case the zero aging period is begun at t_{j-1} and ended at one of the α_js. [see Fig. 3(b)]. In either case, we call the beginning and end ξ_{1_j} and ξ_{2_j}, respectively.

We have defined $t_N = G(t_0)$. We also know that an $\frac{1}{m}$-voltine life cycle exists if $t_N = m + t_0$. Hence if $G(t_0) = m + t_0$, then we must have an $\frac{1}{m}$-voltine solution for t_0. Here we are interested in univoltine life cycles ($m = 1$), and therefore look for t_0 such that the curves $t_N = G(t_0)$ and $t_N = 1 + t_0$ cross (see Fig. 4). If the temperature never falls below the developmental threshold then a univoltine solution can be shown to exist; the argument used by Powell *et al.* (2000) uses

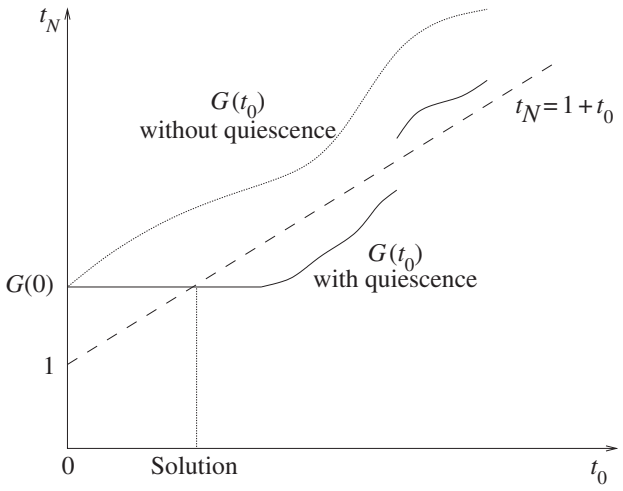

Figure 4. Crossing of $G(y_0)$ and $t_N = 1 + t_0$. The dotted curve is $G(t_0)$ without any quiescence and the solid curve is $G(t_0)$ with quiescence. When quiescence is added, then $G(t_0)$ and t_N are more likely to cross, but discontinuities are induced.

continuity and the conditions

$$G(0) > 1 \qquad \text{and} \qquad G'(t_0) < 1$$

to establish sufficient conditions for existence. However, when temperatures pass below threshold, $G(t_0)$ need not be continuous. While quiescence caused by life-stage specific developmental temperature thresholds may make solutions possible (as in Fig. 4), a continuity-based argument cannot be used to show this.

If $G(0)$ is only slightly larger than 1, quiescence increases the likelihood of a crossing because of the regions with zero slope (see Fig. 4). Such flat regions result from t_0 beginning when temperature is below θ_1 (speed bump); when the egg is laid, the egg immediately enters quiescence and no development occurs until the temperature rises above θ_1. Two eggs laid at different times but both while $T(t) < \theta_1$ will be the same age when they leave dormancy and will therefore have the same emergence date, t_N. Discontinuities in $G(t_0)$ occur when quiescence causes two insects that are similar in initial age to diverge, having very different emergence dates, and may make crossings impossible. To see how discontinuous jumps occur, consider two beetles developing in life stage j only one day apart in age. The first beetle ends life stage j and molts into life stage $j + 1$. Then temperature falls below the developmental threshold for life stage j, causing the second beetle to become quiescent. The first beetle continues to develop, causing the two beetles to have very different emergence dates, t_N. The situations is analogous to traffic flow near a stop light. Initially close cars can be separated by a red signal occurring just between them; similarly, initially distant cars are brought together during a stop signal. The *same* signal causes both phenomena. Overall, then, there

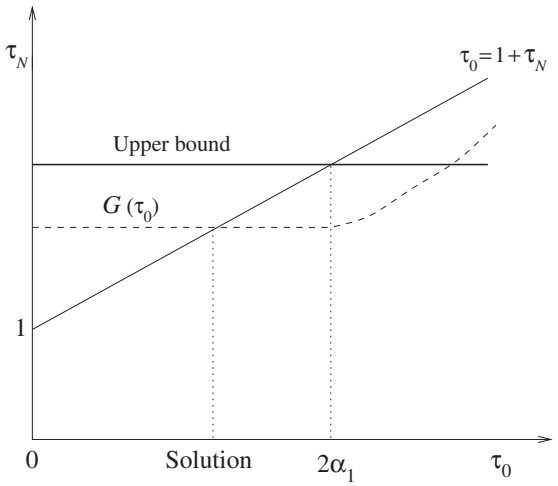

Figure 5. This figure shows the crossing of $\tau_N = 1 + \tau_0$ and $t_N = G(\tau_0)$. The function $G(\tau_0) > 1$ and the upper bound on $G(\tau_0)$ crosses $\tau_N = 1 + \tau_0$ at $\tau_0 = 2\alpha_1$ forcing a crossing in the region of $G(\tau_0)$ with zero slope.

are two competing effects: regions of $G(t_0)$ with zero slope which serve to increase the likelihood of $t_N = G(t_0)$ and $t_N = 1 + t_0$ crossing, and discontinuities in $G(t_0)$ which reduce the likelihood of crossing. For temperatures which make the quiescent stage long enough, solutions (t_0, t_N) for $t_N = 1 + t_0 = G(t_0)$ can be shown to exist, as we will see in the next section.

3. *N* LIFE STAGES

A univoltine solution exists if the curves $t_N = G(t_0)$ and $t_N = 1 + t_0$ cross. To demonstrate this, we will show that t_N has an upper bound for $t_0 < \alpha_1$ and that $t_N = G(t_0)$ is between 1 and the upper bound when $t_0 < \alpha_1$, forcing a crossing (see Fig. 5). It is possible that crossings exist for other values of t_0 (in fact, our numerical results indicate that this is, indeed, the case), but we will show that there exists at least one t_0 that generates a univoltine life cycle for a neighborhood of temperatures. By restricting attention to the interval prior to $t = \alpha_1$ (the beginning of development) we avoid the discontinuities discussed previously.

Traditionally generation length is measured from the egg to the egg in the next generation. We could just as easily define the generation time from the completion of any life stage to the completion of that life stage in the next generation, e.g., first larval instar to first larval instar, or pupae to pupae. Here we choose to define generation time by the life stage with the *highest* developmental threshold. If the temperature is at its minimum during the life stage with the maximum developmental threshold, then individuals in the other life stages will not experience dormancy in a univoltine life cycle, simplifying the problem. In addition, the life stage with

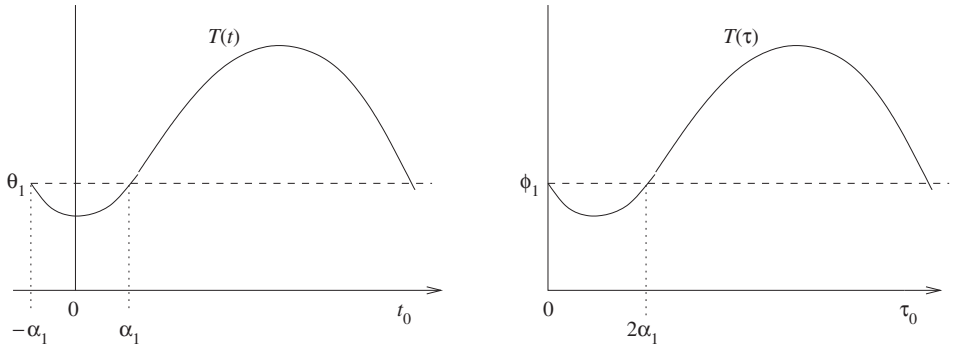

Figure 6. This figure shows how time is shifted so that zero occurs when dormancy begins for the life stage with the highest developmental threshold.

the highest developmental threshold has the longest period of quiescence, maximizing the duration of $G(t_0)$ with zero slope. For example, with MPB the pupal stage has the highest developmental threshold, so we reorganize the life stages such that

$$\phi_1 = \theta_6, \qquad \phi_2 = \theta_7, \qquad \phi_3 = \theta_1, \ \ldots \ , \phi_7 = \theta_5$$

and

$$\rho_1 = r_6, \qquad \rho_2 = r_7, \qquad \rho_3 = r_1, \ \ldots \ , \rho_7 = r_5.$$

Now ϕ_i are the newly ordered developmental thresholds and ρ_i are the reordered linear developmental rates, with i beginning with the highest developmental threshold and continuing through the other $N - 1$ life stages in sequential order. In addition, we reset the clock so that time begins at the point where temperature passes below the first (and highest) developmental threshold. In Fig. 6, the plot on the left shows time and temperature prior to reorganization. The figure on the right shows a new timescale with $\tau = t + \alpha_1$ and $T(t) = T_0 - T_1 \cos(2\pi(\tau - \alpha_1))$ with $\tau = 0$ at the former $t = -\alpha_1$. Hence τ_0 is the time the insect begins the stage with the highest developmental threshold and τ_N is the time the insect finishes the life stage just prior to the one with the highest developmental threshold and begins a new generation. In MPB, τ_0 is the inception of the pupal life stage and τ_7 is the time of completion of the fourth larval instar.

The aging equations (1) become

$$1 = \int_{\tau_{j-1}}^{\tau_j} \max[0, \rho_j(T(\tau) - \phi_j)] \, d\tau.$$

Suppose $\tau_0 \in [0, 2\alpha_1]$. No development occurs until $\tau > 2\alpha_1$, and consequently aging in the initial stage satisfies

$$\frac{1}{\rho_1} = \int_{2\alpha_1}^{\tau_1} [T_0 - T_1 \cos(2\pi(\tau - \alpha_1)) - \phi_1] \, d\tau$$

$$= (T_0 - \phi_1)(\tau_1 - 2\alpha_1) - \frac{T_1}{2\pi}(\sin(2\pi(\tau_1 - \alpha_1)) - \sin(2\pi\alpha_1)). \qquad (9)$$

Define α_2 to be the time at which temperatures cross the second highest threshold, that is, $\alpha_2 = \frac{1}{2\pi}\cos^{-1}\left(\frac{T_0-\phi_{\text{submax}}}{T_1}\right)$ and $\phi_{\text{submax}} = \max_{2\le j\le N}\{\phi_j\}$. If

$$t_N = \tau_N - \alpha_1 \le 1 - \alpha_2, \qquad (\tau_N \le 1 + \alpha_1 - \alpha_2),$$

then no other development thresholds are crossed during a univoltine life cycle (thus avoiding discontinuities). The remaining equations for development can then be written

$$\frac{1}{\rho_j} = (T_0 - \phi_j)(\tau_j - \tau_{j-1}) - \frac{T_1}{2\pi}(\sin(2\pi(\tau_1 - \alpha_1)) - \sin(2\pi(\tau_{j-1} - \alpha_1))). \quad (10)$$

Summing (9) and (10), we get

$$\sum_{j=1}^{N}\frac{1}{\rho_j} = T_0(\tau_N - 2\alpha_1) - \tau_N\phi_N + 2\alpha_1\phi_1 + A$$

$$+\frac{T_1}{2\pi}(\sin(2\pi\alpha_1) - \sin(2\pi(\tau_N - \alpha_1))),$$

where

$$A \stackrel{\text{def}}{=} \sum_{j-1}^{N}\tau_j(\phi_{j+1} - \phi_j).$$

We are interested in $\tau_N \in [1, 1 + \alpha_1 - \alpha_2)$, that is, times of completion satisfying $G(\tau_0) > 1$ but avoiding discontinuities, so we write

$$\tau_N = 1 + \alpha_1 - \delta, \qquad \delta \in (0, \alpha_2).$$

Now we estimate

$$\sin(2\pi(\tau_N - \alpha_1)) = \sin(2\pi(1 - \delta)) \ge \sin(2\pi) - 2\pi\delta\cos(2\pi) = -2\pi\delta$$

using Taylor's theorem. It follows that

$$-\frac{T_1}{2\pi}\sin(2\pi(\tau_N - \alpha_1)) \le \frac{T_1}{2\pi}2\pi\delta = T_1\delta = T_1(1 + \alpha_1 - \tau_N).$$

Therefore,

$$\sum_{1}^{N}\frac{1}{\rho_j} \le (T_0 - \phi_N)\tau_N - 2\alpha_1 T_0 + A + \frac{T_1}{2\pi}\sin(2\pi\alpha_1) + T_1(1 + \alpha_1 - \tau_N)$$

$$= \tau_N(T_0 - \phi_N - T_1) + A + T_1(1 + \alpha_1) - 2\alpha_1 T_0 + \frac{T_1}{2\pi}\sin(2\pi\alpha_1).$$

(11)

Table 1. Parameters for linearized rates of development for mountain pine beetle, including developmental thresholds, θ_j. Temperatures are measured in degrees centigrade, while developmental rates, r_j, have units of inverse degrees per year (Powell *et al*., 2000).

Developmental stage	Developmental threshold	Linear rate
Egg	$\theta_1 = 7.5394$	$r_1 = 4.1975$
First larval instar	$\theta_2 = 8.6358$	$r_2 = 10.6945$
Second larval instar	$\theta_3 = 9.6322$	$r_3 = 10.4390$
Third larval instar	$\theta_4 = 8.0342$	$r_4 = 3.4675$
Fourth larval instar	$\theta_5 = 10.9543$	$r_5 = 3.6500$
Pupae	$\theta_6 = 11.7555$	$r_6 = 6.2780$
Ovipositional adult	$\theta_7 = 1.7929$	$r_7 = 1.2775$

In general, $T_0 - \phi_N - T_1 < 0$, so if we solve (11) for τ_N we get an upper bound

$$\tau_N \leq \frac{A + T_1(1+\alpha_1) - 2\alpha_1 T_0 + \frac{T_1}{2\pi}\sin(2\pi\alpha_1) - \sum_{j=1}^{N}\frac{1}{\rho_j}}{T_1 + \phi_N - T_0}. \tag{12}$$

Finally, we must find an overestimate for A. If $\phi_j - \phi_{j-1} < 0$ we define $D_j \stackrel{\text{def}}{=} \phi_j - \phi_{j-1}$, and if $\phi_j - \phi_{j-1} > 0$ we define $U_j \stackrel{\text{def}}{=} \phi_j - \phi_{j-1}$. Because we do not know how many $(\phi_j - \phi_{j-1})$'s will be positive and how many will be negative, we have to bound both $\sum_j \tau_j D_j$ and $\sum_j \tau_j U_j$ independently.

Let $\bar{\phi} = \frac{1}{N}\sum_{j=1}^{N}\phi_j$ be the average threshold. The D_j are negative, and the maximum threshold, ϕ_1, is subtracted in D_1, therefore $\sum_j D_j \leq (\bar{\phi} - \phi_1)$. Also, since ϕ_1 is subtracted, $\sum_j U_j \leq (\phi_{\text{submax}} - \phi_{\text{min}})$, when ϕ_{min} is the lowest threshold. (For MPB, $\phi_{\text{max}} = \phi_1$, $\phi_{\text{submax}} = \phi_N$ and $\phi_{\text{min}} = \phi_2$, see Table 1). Since $\tau_1 > 2\alpha_1$ and $\tau_j < \tau_N$, for $j < N$

$$A < 2\alpha_1(\bar{\phi} - \phi_1) + \tau_N(\phi_N - \phi_{\text{min}}). \tag{13}$$

Using (8) and trigonometric properties, we replace $\frac{T_1}{2\pi}\sin(2\pi\alpha_1)$ with $\frac{1}{2\pi}\sqrt{T_1^2 - (\phi_1 - T_0)^2}$ and substitute (13) for A in (12). Solving for τ_N, we get

$$\tau_N \leq \frac{T_1(1+\alpha_1) - 2\alpha_1(T_0 + \phi_1 - \bar{\phi}) + \frac{1}{2\pi}\sqrt{T_1^2 - (\phi_1 - T_0)^2} - \sum_{j=1}^{N}\frac{1}{\rho_j}}{T_1 + \phi_N - T_0 - \phi_{\text{submax}} + \phi_{\text{min}}}. \tag{14}$$

In the particular case of MPB developmental thresholds the denominator becomes $T_1 - T_0 + \phi_2$.

It remains to show that this bound can be used to guarantee crossings. As $T_1 \longrightarrow (\phi_1 - T_0)$, $\alpha_1 \longrightarrow 0$, and

$$\tau_N \longrightarrow \frac{\phi_1 - \sum_{j=1}^{N}\rho_j - T_0}{\phi_1 - 2T_0 + \phi_2} = \frac{1}{2} \qquad \text{as} \qquad T_0 \longrightarrow \infty.$$

Thus, the bound on τ_N can be made less than 1 for sufficiently large T_0. As $T_1 \longrightarrow \infty$, on the other hand, $\alpha_1 \longrightarrow \frac{1}{4}$ and the bound tends to $1 + \alpha_1 + \frac{1}{2\pi} = \frac{5}{4} + \frac{1}{2\pi}$. In this case, $1 + \alpha_1 - \alpha_2 \longrightarrow 1 + \frac{1}{4} - \frac{1}{4} = 1$. Since the bound is less than $1+\alpha_1-\alpha_2$ for $T_1 \longrightarrow (\phi_1 - T_0)$ and greater than 1 for $T_1 \longrightarrow \infty$, there must exist a range of T_1 that satisfy $\tau_N \in (1, 1 + \alpha_1 - \alpha_2) \subset (1, 1 + 2\alpha_1)$, which implies that a univoltine solution exists for some range of temperatures. The predicted temperature region from equation (14) that supports univoltinism is depicted in relation to simulation data for MPB in Fig. 7.

These univoltine solutions will be extremely stable, dynamically, since they are constructed so that $G'(t_0) = 0$ for $t_0 \in (-\alpha_1, \alpha_1)$. In fact, the univoltine points are so stable that nearby points converge to them super-exponentially (i.e., in a finite number of iterations) in subsequent generations. A more difficult question is the structural stability of the univoltine orbits. An orbit is structurally stable when it is observable in an open set of parameters, including parameters specifying the current model among structurally 'nearby' models in which it is nested. This must be demonstrated because the simple, linear development hypothesis (3) is very restrictive, but central to our existence proof. Without structural stability we can not expect these results to persist for real, nonlinear insect development. One approach to demonstrating structural stability is to show that the orbit results from transverse intersection of differentiable manifolds.

The univoltine cycles described above are points of intersection of the surfaces (6)

$$1 = f_j(t_{j-1}, t_j), \qquad j = 2, 3, \ \ldots, \ N - 1,$$

the surface

$$1 = f_1(\alpha_1, t_1),$$

and the surface

$$1 = f_N(t_{N-1}, 1 + t_0). \tag{15}$$

The f_j are integrals of developmental rates, as in (7), and in equation (15) we have used $t_N = 1 + t_0$ for the univoltine cycle. Let $\mathbf{t}^* = (t_0^*, t_1^*, \ldots, t_{N-1}^*)^T$ denote the vector of start times for life stages in the univoltine cycle. From the definition of f_j,

$$\frac{\partial}{\partial x} f_j(x, y) = -\frac{\partial}{\partial x} f_j(y, x),$$

and

$$\frac{\partial}{\partial t_j} f_j(t_{j-1}^*, t_j^*) = 0 \qquad \text{only if} \qquad T_0 - \theta_j = T_1 \cos(2\pi t_j^*).$$

This latter condition only happens if temperatures pass below threshold precisely as the individual molts to successive life stages. This, in turn, is impossible since no development occurs at or below threshold. Thus, if we define

$$\nabla = (\partial_{t_0}, \partial_{t_1}, \ldots, \partial_{t_{N-1}})^T$$

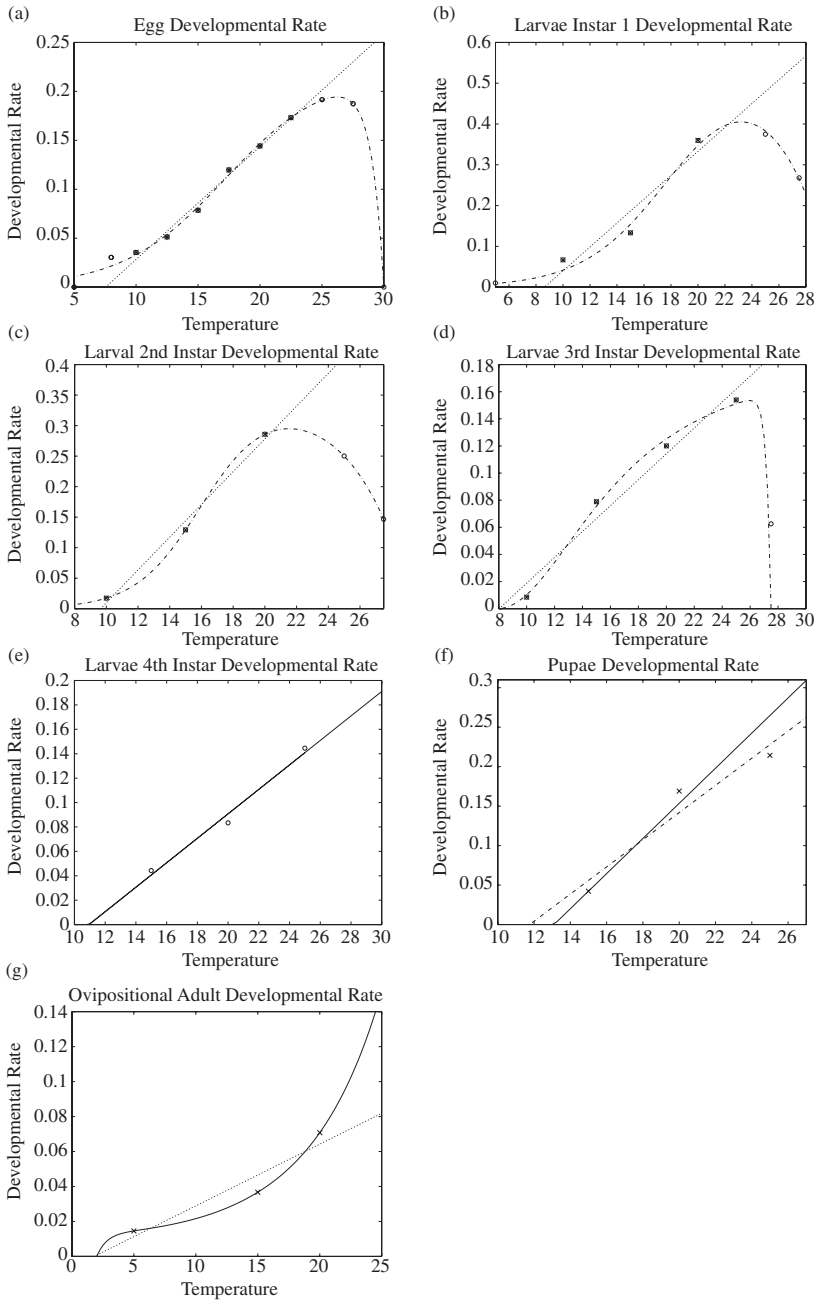

Figure 7. Nonlinear rate curves for MPB (solid) and linear approximations (dashed) with developmental thresholds and linear rates of development. From left to right, top to bottom the curves represent rates of development for (a) eggs; (b) first larval instar; (c) second larval instar; (d) third larval instar; (e) fourth larval instar; (f) pupae; and (g) ovipositional adults. Open circles represent developmental data, while '$\times$' represent observed data selected to parametrize a purely linear representation of the developmental rate.

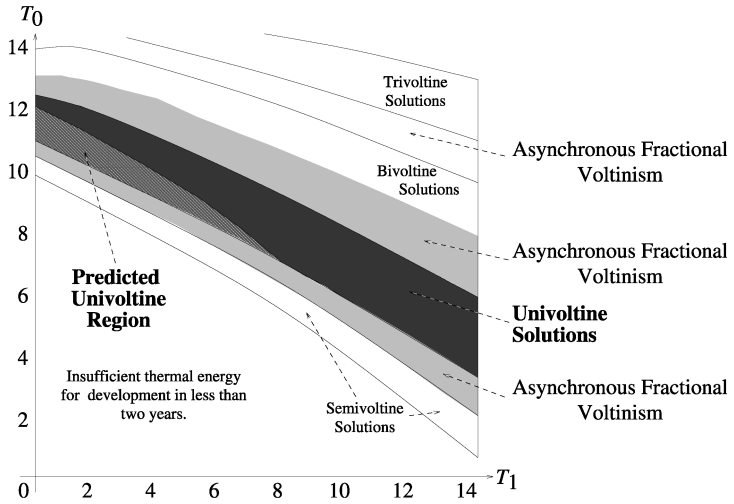

Figure 8. Combinations of mean annual temperatures in degrees centigrade, T_0, and seasonal fluctuations in degrees centigrade, T_1, for which equation (14) predicts univoltine life cycles for mountain pine beetle. Predicted univoltine region using (14) is depicted as a cross-hatched region. The true univoltine solutions for the nonlinear phenology model inhabit the darkly shaded area, in which the prediction is imbedded. Above and below the firmly univoltine region are regions in which solutions of fractional voltinism (lightly shaded) are possible, as shown in more detail in other simulation figures.

and denote non-zero entries by '♠', we get

$$\nabla f_j(\mathbf{t}^*) = (\underbrace{0, 0, \ldots, 0}_{j-2}, \spadesuit, \spadesuit, \underbrace{0, 0, \ldots, 0}_{N-j})^T, \qquad j = 2, 3, \ldots, N-1,$$

$$\nabla f_1(\mathbf{t}^*) = (0, \spadesuit, 0, 0, \ldots, 0)^T \qquad \text{and}$$

$$\nabla f_N(\mathbf{t}^*) = (\spadesuit, 0, 0, \ldots, 0, \spadesuit)^T$$

when evaluated at $(t_0^*, t_1^*, \ldots, t_{N-1}^*)$. Notice that the position of the non-zero entries differs for the gradient of each function, and therefore $\nabla f_j(\mathbf{t}^*)$ cannot be parallel to $\nabla f_k(\mathbf{t}^*)$ for any $j \neq k$ at $\mathbf{t}^*$; the surfaces intersect transversely. Consequently, the univoltine cycles are structurally stable. In the next section we will test structural stability by searching for univoltine cycles in linear and nonlinear developmental models for MPB.

4. APPLICATION TO MPB

Mountain pine beetles show no evidence of diapause, yet maintain synchrony and appropriate seasonality. Figure 8 shows the actual developmental rate curves

for MPB estimated previously (Logan and Amman, 1986; Bentz *et al*., 1991; Logan and Bentz, 1999) along with linear approximations of these curves (Powell *et al*., 2000). Determining true development thresholds for this insect in laboratory experiments has proven difficult. Larvae feed and develop within the cryptic habitat of tree phloem. It is extremely difficult to maintain an appropriate environment for the length of time required to monitor development at low temperatures. Due to these problems, current best estimates of low-temperature developmental thresholds for this insect are those derived by linearly projecting the lowest developmental rates. The parameter values for the linear model appear in Table 1.

By iterating the ovipositional map for many generations we are able to determine which seasonal cycles, if any, are attracting. Structural stability of our predictions will be tested both by investigating the nonlinear development model as well as adding complications (realism) to the temperature profile. For the case with daily temperature fluctuations the temperatures will be modeled using the truncated Fourier series

$$T(t) = T_0 - T_1 \cos(2\pi t) - T_{365} \cos(730\pi t).$$

In this series T_0 represents the mean annual temperature, T_1 is the amplitude of the seasonal fluctuation between summer and winter average temperatures, and T_{365} is average amplitude of oscillation between daily highs and lows. We set $T_{365} = 0$ for simulations which have only seasonal temperature fluctuations. Equations (1) were integrated using the trapezoid rule in MATLAB with arbitrarily chosen initial conditions, t_0, for at least 100 generations of developmental time, and the emergence date for the median individual for each year was recorded. This sequence of median ovipositional dates were examined for seasonality. Seasonality is achieved if after a 'few' years, the emergence date remains the same for all following years.

For each choice of T_0, T_1 the number of generations per year at the end of the simulation was also recorded. A contour plot of the voltinism for seasonal fluctuations only ($T_{365} = 0$) is presented in Fig. 9. The white areas are regions of stable voltinism. The black and white marbled areas are regions of fractional or asynchronous voltinism. Such voltinism occurs if stable orbits do not exist or if for such a stable orbit the number of generations per year *or* number of years per generation is not a whole number, e.g., 1.7 generations per year. Thus one generation every 2 years (semi-voltinism) is not asynchronous, but three generations every 2 years would be. Though MPB generally live in temperate environments, they require an adequate amount of thermal energy for development. Figure 9 illustrates this; if the mean annual temperature (T_0) is high, then only small seasonal fluctuations are required to achieve univoltine life cycles. However, if the mean annual temperature is low, then large seasonal temperature fluctuations are required to acquire enough thermal energy for development through all seven life stages. Figure 7 shows the temperature region predicted by equation (14) to sup-

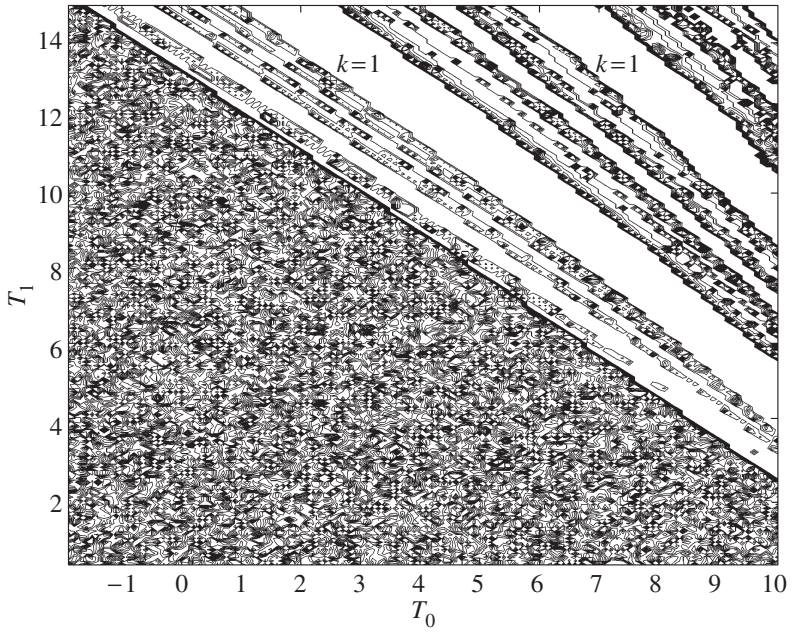

Figure 9. Combinations of mean annual temperature, T_0, and seasonal fluctuation in degrees centigrade, T_1, for which the model using linear approximations to developmental rate curves predicts k-voltine life cycles. The white areas are regions of stable voltinism. The black and white marbled areas are regions of asynchronous fractional voltinism. Where $k = 1$, univoltinism (one generation per year) is supported. The regions of temperature where $k = 2$ support two generations per year for MPB. A narrow band of semi-voltine solutions exist ($k = \frac{1}{2}$) for cooler temperatures, but is not labelled.

port univoline life cycles. Some of this predicted region coincides with predicted regions for univoltinism from the simulations (shown in Fig. 9).

Figure 10 depicts the regions of voltinism when daily fluctuations are included ($T_{365} \neq 0$). In this case $T_0 = 3$ °C. Daily fluctuations reduce the size of seasonal fluctuations required for successful synchrony. This occurs because beetles acquire more energy on some days due to daily temperature fluctuations. The lower bound for T_1 is decreased, generating a larger set of temperatures which create stable univoltine life cycles, increasing the success of MPB.

In Figure 9 the bands of stable voltinism are separated by regions of asynchronous fractional voltinism. It has been hypothesized (Logan and Bentz, 1999) that an increase in mean annual temperature from inside to outside the regions of voltinism destabilizes life cycles before the temperature reaches another region of stable integer voltinism. This would lead to a disruption in synchrony, limiting MPB distribution. For organisms with many life stages, development may be approximated by linear rate curves (Powell *et al*., 2000), however, Logan *et al*. (1976) (and others before) provide evidence that arthropods have nonlinear developmental rate

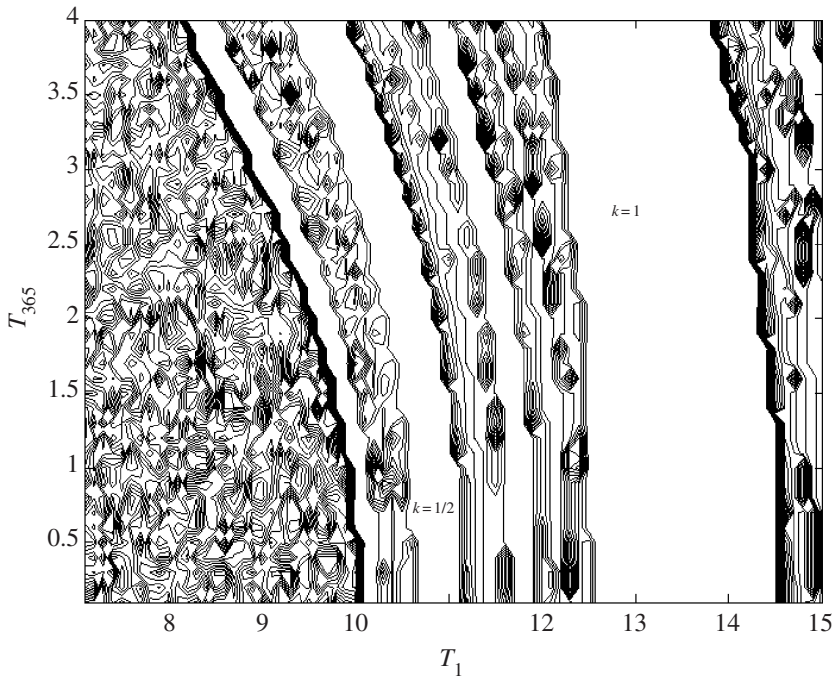

Figure 10. Voltinism generated by combinations of seasonal temperature fluctuations, T_1, and daily temperature fluctuations, T_{365}, when the mean annual temperature, $T_0 = 3\ ^\circ\mathrm{C}$ degrees centigrade. The k-voltine cycles are predicted using linear approximations to developmental rate curves. The white areas are regions of stable voltinism. The black and white marbled areas are regions of asynchronous fractional voltinism. Note the broadened band of semi-voltine solutions ($k = \frac{1}{2}$).

curves. Table 2 shows the functional forms for developmental rate curves depicted in Fig. 8, followed by parameter values for the nonlinear rate curves in Table 3. As a test of the predicted structural stability of our results we repeat the previous numerical experiments using nonlinear rate curves for MPB.

Figure 11 shows that the nonlinear developmental rate functions decrease the size of temperature regions for which integer voltinism is achieved as compared with the linear curves in Fig. 9. Regions of asynchronous fractional voltinism separating regions of stable voltinism are not removed. Contrary to the model outcome using linear developmental rate curves, when daily fluctuations are added to the model with nonlinear developmental rate curves, the regions of stable voltinism are decreased (see Fig. 12). This is due to the modal nonlinear developmental rate curves (see Fig. 8). At moderate temperatures the linear model overestimates the amount of development occurring in the first four life stages. The linear rate curves increase as temperature increases, whereas the nonlinear rate curves have a peak in the 20's and then decrease as temperature continues to rise. In the 20's, however, the nonlinear rate curves are underestimated by the linear approxima-

Table 2. Functional forms for nonlinear development (Logan, 1988) for mountain pine beetles. The functional form for each of the life stages is used if the development is positive, otherwise the rate is set to zero. Thresholds are implemented in the third larval stage and the ovipositional adult stage by the additional requirement that the temperature must be above the developmental threshold, p_5, or else rates are set to zero.

Developmental stage	Functional forms for $T > 0$
Egg	$p_1\left[\frac{1}{1+p_2\exp(-p_3(T-5))} - \exp\left(\frac{-p_4+T+5}{p_5}\right)\right]$
First larval instar	$p_1\left[\frac{1}{1+p_2\exp\{-p_3(T-5)\}} - \exp\left(\frac{-p_4+T+5}{p_5}\right)\right]$
Second larval instar	$p_1\left[\frac{1}{1+p_2\exp\{-p_3(T-10)\}} - \exp\left(\frac{-p_4+T+5}{p_5}\right)\right]$
Third larval instar	$p_1\left[\left(1+\left(\frac{p_4}{T-p_5}\right)^2\right)^{-1} - \exp\left(\frac{T-p_2-p_5}{p_3}\right)\right]$
Fourth larval instar	$p_1(T-p_2)$
Pupae	$p_1(T-p_2)$
Ovipositional adult	$2.54\ p_1\left[\exp\left(p_2(T-p_5)^{p_3}\right) - \exp\left(\frac{p_5-T}{p_4}\right)\right]$

Table 3. Parameters for nonlinear rates of development for mountain pine beetle.

Developmental stage	p_1	p_2	p_3	p_4	p_5
Egg	114.9020	19.9353	0.2034	29.6029	4.8851
First larval instar	251.3755	57.2790	0.3004	25.2244	4.5963
Second larval instar	130.0130	18.0117	0.4788	19.3602	3.4696
Third larval instar	69.6785	19.7005	0.1542	8.7683	7.9046
Fourth larval instar	3.6500	10.9543			
Pupae	6.2780	11.7555			
Ovipositional adult	61.6850	0.0194	1.5400	0.8000	2.0000

tion. Consequently bands of tri-voltine solutions are depicted in Fig. 11, which do not appear in the corresponding figure for linear rate curves (Fig. 9). For very high temperatures in the linear model, beetles age rapidly, while in the nonlinear model beetles do not develop as much (past the mode optimal development temperatures). Thus, for very high temperatures the linear model predicts regions of high voltinism, which are never observed. However, this is far from the regime in which the linear model can be expected to be any kind of approximation to reality. For our purposes, the overall structural correspondence between the linear model predictions and the nonlinear phenology simulations is very good, as predicted by structural stability.

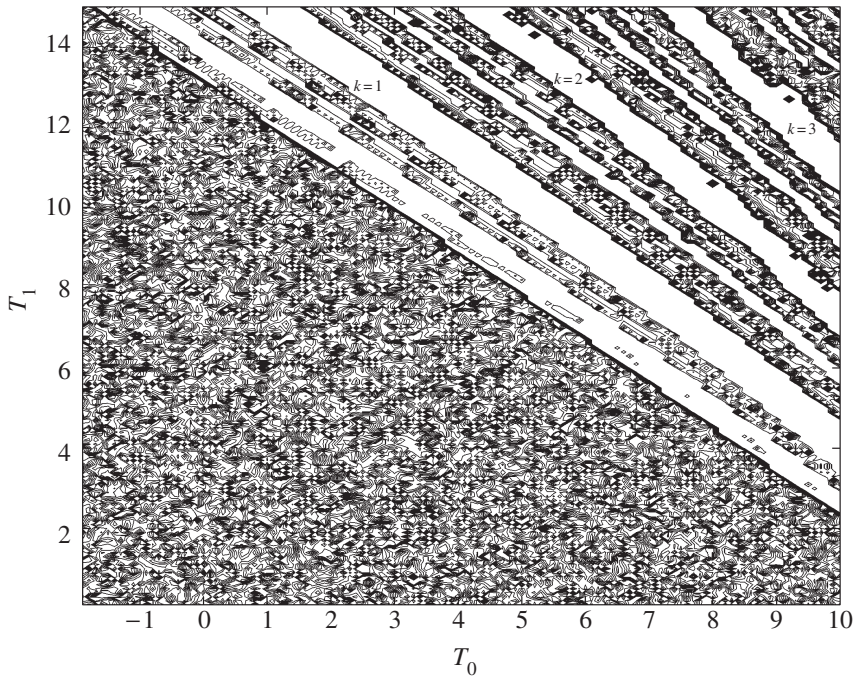

Figure 11. Voltinism generated by combinations of mean annual temperature, T_0, and seasonal temperature fluctuations, T_1, using nonlinear development rate curves. Predicted k-voltine life cycles (in white) are separated by black and white marbled regions of asynchronous fractional voltinism. There are temperatures for which uni-($k = 1$), bi-($k = 2$), and tri-($k = 3$)voltine life cycles are supported. A narrow band of semi-voltine ($k = \frac{1}{2}$) solutions exists for low temperatures, but is not labelled.

5. CONCLUSIONS

Seasonal timing and synchrony are vital to the survival and reproduction of MPB. We see that yearly temperature variations alone are enough to create conditions for univoltine life cycles, promoting an adaptive seasonality. Furthermore, periods in the life cycle during which an insect is in a quiescent state enhance integer voltinism. As seen in the simulations, bivoltine (and multivoltine) life cycles are also possible when enough thermal energy exists in the system, i.e., high mean annual temperature with large seasonal fluctuations. For organisms with one high developmental threshold these cyclic solutions are structurally stable, and therefore likely to be observed.

In this paper we have shown that univoltine solutions exist for reasonable temperature regimes as suggested by Logan and Bentz (1999). There are, however, many possible fixed points for the system, not all of which are univoltine. As seen in simulations, suitable conditions for univoltinism are fairly restricted. Some modification in the temperature, two degrees in either mean or seasonal temperatures

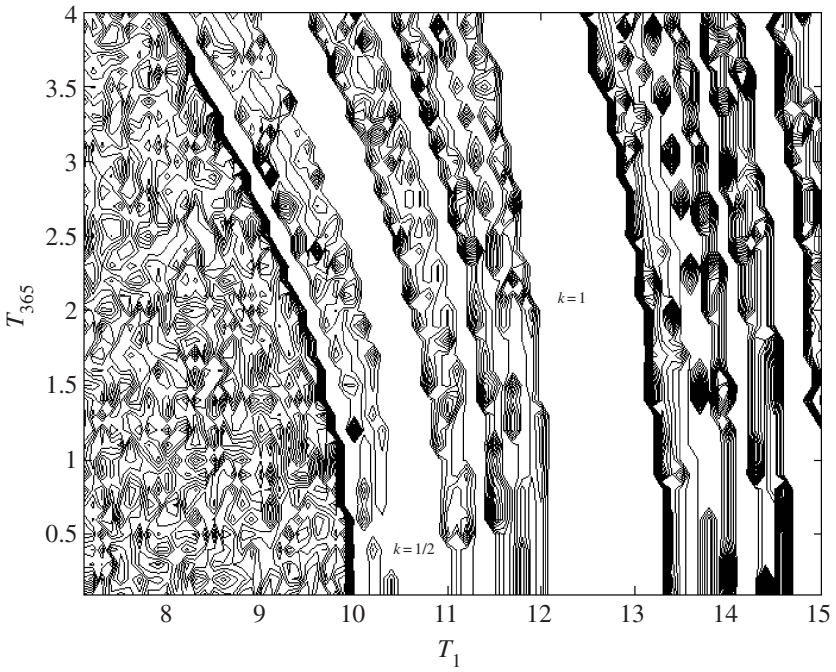

Figure 12. Voltinism generated by combinations of seasonal temperature fluctuations, T_1, and daily temperature fluctuations, T_{365}, when the mean annual temperature is $T_0 = 3\,^{\circ}\mathrm{C}$. Nonlinear rate curves generate k-voltine cycles (white), separated by marbled regions of asynchronous fractional voltinism. The white band to the far right of the figure is a band of bi-voltine solutions. Note the broadened band of semi-voltine solutions ($k = \frac{1}{2}$) which exists for lower temperatures.

(such as could occur from global warming) may alter or destroy the current voltinism that allows MPB to be successful, thrusting MPB into regimes of asynchronous fractional voltinism. Conversely, the same warming could make new regions accessible to MPB (e.g., Jack pines in Canada) which are currently protected by the thermal prohibition of asynchronous or fractional voltinism. This model could be used to determine what habitats, based on temperature, MPB may inhabit. In addition, due to the generality of the mechanisms we consider, these sorts of predictions may be applicable to other temperate insects without diapause, enhancing general understanding of insects under direct temperature control.

ACKNOWLEDGEMENTS

This work was supported, in part, by the National Science Foundation under grant number DMS-0077663, for which the authors are grateful. J. Jenkins was also supported by the USDA Forest Service Mountain Pine Beetle Project through grant number RMRS-99612-RJV.

REFERENCES

Amman, G. D. and W. E. Cole (1983). Mountain pine beetle dynamics in lodgepole pine forests part II: population dynamics. *USDA For. Serv. Gen. Tech. Rpt. INT-145*.

Bentz, B. J., J. A. Logan and G. D. Amman (1991). Temperature-dependent development of the mountain pine beetle (*Coleoptera: Scolytidae*) and simulation of its phenology. *Can. Entomol.* **123**, 1083–1094.

Bentz, B. J. and D. Mullen (1999). Ecology of mountain pine beetle (Coleoptera: Scolytidae) cold hardening in the Intermountain West. *Environ. Entomol.* **28**, 577–587.

Danks, H. V. (1987). *Insect Dormancy: An Ecological Prospective*, Monograph Series No.1. Biological Survey of Canada (Terrestrial Arthropods), Ottawa.

Grist, E. P. M. and W. S. C. Gurney (1995). Stage-specificity and the synchronisation of life-cycles to periodic environmental variations. *J. Math. Biol.* **34**, 123–147.

Gurney, W. S. C., P. H. Crowley and R. M. Nisbet (1992). Locking life cycles onto seasons: circle-map models of population dynamics and local adaptation. *J. Math. Biol.* **30**, 251–279.

Gurney, W. S. C., P. H. Crowley and R. M. Nisbet (1994). Stage-specific quiescence as a mechanism for synchronizing life cycles to seasons. *Theo. Pop. Biol.* **46**, 319–343.

Logan, J. A. (1988). Toward an expert system for development of pest simulation models. *Environ. Entomol.* **17**, 359–376.

Logan, J. A. and G. D. Amman (1986). A distribution model for egg development in mountain pine beetle. *Can Entomol.* **118**, 361–372.

Logan, J. A. and B. J. Bentz (1999). Model analysis of mountain pine beetle (*Coleoptera: Scolytidae*) seasonality. *Environ. Entomol.* **28**, 924–934.

Logan, J. A. and J. A. Powell (2001). Global warming, ghost forests, and mountain pine beetles. Submitted to *American Entomologist*.

Logan, J. A., D. J. Wollkind, S. C. Hoyt and L. K. Tanigoshi (1976). An analytic model for description of temperature dependent rate phenomena in arthropods. *Environ. Entomol.* **5**, 1133–1140.

Newbold, J. D., B. W. Sweeney and R. L. Vannote (1994). A model for seasonal synchrony in stream mayflies. *J. North Am. Benthological Soc.* **13**, 3–18.

Powell, J. A., J. L. Jenkins, J. A. Logan and B. J. Bentz (2000). Seasonal temperatures alone can synchronize life cycles. *Bull. Math. Biol.* **62**, 977–998.

Raffa, K. F. (1988). The mountain pine beetle in Western North America, in *Dynamics of Forest Insect Populations Patterns, Causes, Implications*, A. A. Berryman (Ed.), Pullman, Washington: Washington State University, pp. 506–525.

Raffa, K. F. and A. A. Berryman (1980). Flight responses and host selection by bark beetles, in *Dispersal of Forest Insects: Evaluation, Theory and Management Implications*, A. A. Berryman and L. Safranyik (Eds), Pullman, Washington: Washington State University, pp. 213–233.

Tauber, M. J., C. A. Tauber and S. Masaki (1986). *Seasonal Adaptations of Insects*, New York: Oxford University Press.

Taylor, F. (1981). Ecology and evolution of physiological time in insects. *Am. Nat.* **117**, 1–23.

Zaslavski, V. A. (1988). *Insect Development: Photoperiodic and Temperature Control*, Berlin: Springer.

Received 20 December 2000 and accepted 21 February 2001